Fringe Fitting of VGOS Data for Astrogeodesy

Wara Chamani, Minghui Xu

Abstract Source structure modelling of VLBI global observing system (VGOS) observations is one of the main interests for Astrogeodesy, a project combining the knowledge from geodesy, astrometry and radio astronomy. We report our research on the calibration of a VGOS dataset using astronomical data reduction software. We investigate whether fringe fitting works for VGOS data, identify potential problems in the data that may hinder the amplitude and phase calibrations, and find ways to improve the calibration process.

Keywords VGOS, fringe fitting, source structure

1 Introduction

Astrogeodesy, funded by the Horizon Europe programme, is a new project that aims to help fulfill the VGOS goals. These include 1 mm accuracy and 0.1 mm/year stability in station positions on a global scale. These improvements are very important for the global terrestrial reference frame and celestial reference frame as well as astrophysics. To achieve these accuracies, the effects of source structure on VGOS datasets must be considered before generating geodetic products.

Source structure has been ignored in geodetic Very Long Baseline Interferometry (VLBI) observations, and it is a limiting factor for achieving high-accuracy source and station positions [7]. For example, the systematic errors introduced by source structure have been recently reported to be at the level of 20 picoseconds, which is considered a major systematic error in VGOS observations [1, 6]. VGOS observes and detects radio signals from quasars, a type of Active Galactic Nuclei (AGN), which at radio frequencies and milliarcsecond (mas) scales often exhibit a relativistic plasma jet launched in a certain direction originating from regions near a supermassive black hole residing in the center of the galaxy. Imaging at four different bands spanning from 3.3 to 10.5 GHz confirms the presence of jets in VGOS sources (e.g., 0016+731, 1803+784, 1418+546) as described by [7]. Note that for the goal of 1 mm accuracy the "invisible" structure of the AGNs at the sub-mas scales (i.e., smaller than the beam size) has to be taken into account as well. Correcting the effects of source structure in VGOS observations requires first source structure modelling, i.e., systematically calibrating and imaging ultra-broadband VGOS observations. In this work, the authors focus initially on developing a pipeline to calibrate VGOS observations in an astronomical calibration mode.

Helmholtz-Zentrum, Deutsches GeoForschungsZentrum, Germany

2 Observations and Analysis

We processed one IVS VGOS experiment, session VR2201, observed on January 20–21, 2022. The session involved nine participating antennas: GGAO12M (GS), HOBART12 (HB), KOKEE12M (K2), MACGO12M (MG), ONSA13NE/ONSA13SW (OE and OW), WESTFORD (WF), WETTZ13S (WS), and RAEGYEB (YJ). It was scheduled using the radio-source-centric approach to improve the imaging capability of geodetic observations [5]. The session utilized a 512-MHz-wide bandwidth at each of the four bands: 3 GHz (A-band), 5 GHz (B-band), 6 GHz (C-band), and 10 GHz (D-band), in both vertical and horizontal polarization. Each band is further divided into eight selected channels of a 32-MHz bandwidth.

The raw data were correlated with a spectral window of 0.25 MHz (resulting in 128 points at each 32 MHz channel) and an integration time of one second. The SWIN data provided by the IVS data archive were transformed to circular polarization using the software `Polconvert` [4]. Simultaneous scans (more than one source observed simultaneously) with a lesser number of antennas were then flagged, retaining only the scans with the higher (or highest if more than two sources were observed at the same time) number of antennas. This selective approach was prompted due to the data being grouped into subarrays by the Astronomical Interactive Processing System (`AIPS`), which resulted in many failed solutions in fringe fitting and required several subarrays to be processed separately. After flagging the subarray data, several output FITS files were generated.

We calibrated the data using the `AIPS` software based on the `AIPS` cookbook[1] [3]. A standard calibration of astronomical VLBI data for AGNs includes amplitude and phase calibrations. Our current calibration pipeline is schematically displayed in Figure 1. However, we currently omitted the amplitude calibration because we did not count on TSYS information for this experiment. After loading the generated FITS files, we inspected the visibilities at the four frequency bands for various sources, scans, and baselines to identify outliers.

Overall, we found RFI in the amplitude visibilities between 10.20 and 10.65 GHz in baselines with antenna YJ; see Figure 2 as an example. The RFI in the spectral windows between 3 and 5 at 10.48 GHz was removed from all the scans. Furthermore, an extensive flagging of phase cal tones in baseline OE–OW across all scans and frequencies was conducted. In the first stage of phase cal tone flagging, we removed visibilities from the following spectral windows: 19-20, 39-40, 59-60, 79-80, and 99-100, from frequencies of 3 GHz, 5.24 GHz, 6.36 GHz, and 10.20 GHz. Additionally, we flagged spectral windows 31-32, 51-52, 71-72, 91-92, and 111-112 at frequencies of 3.03 GHz, 3.19 GHz, 3.35 GHz, 5.27 GHz, 5.43 GHz, 5.59 GHz,

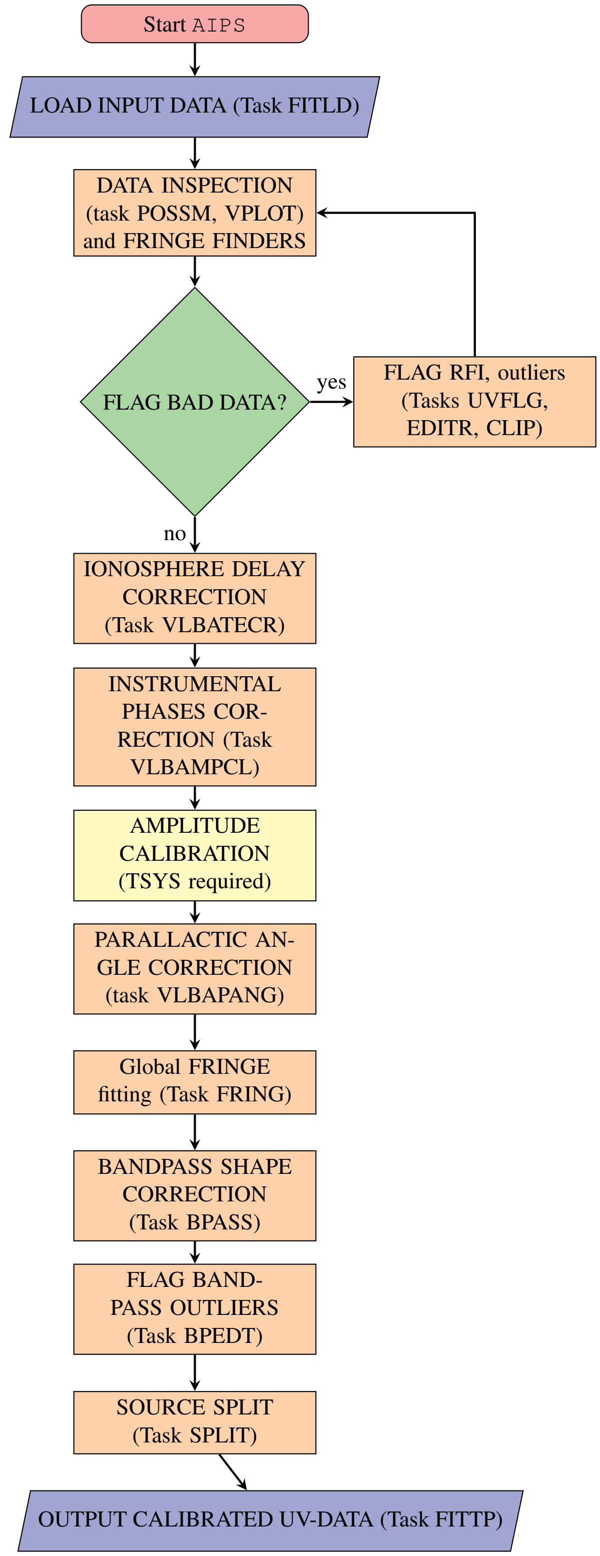

Fig. 1 Flowchart of the current calibration pipeline of VGOS data in `AIPS`. This does not include amplitude calibration for session VR2201, as no TSYS information is available.

[1] http://www.aips.nrao.edu/cook.html

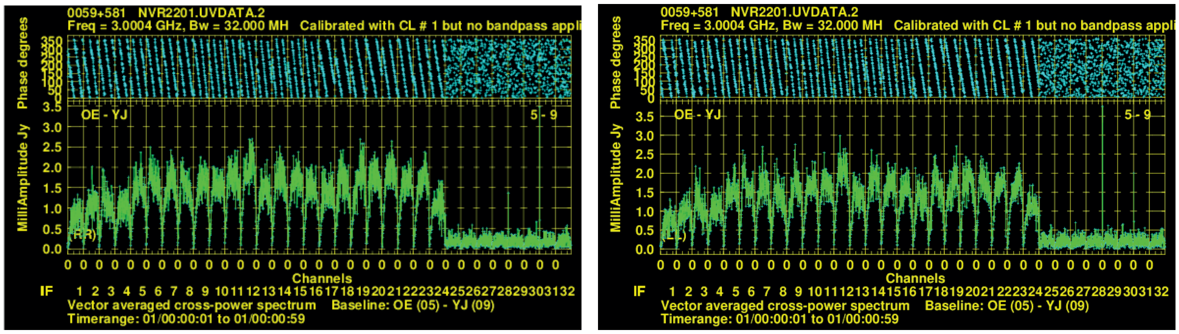

(a) (b)

Fig. 2 Amplitude (lower panel) and phase (upper panel) visibilities of source '0059+581' in a one-minute scan observed at frequencies from 3 to 10.6 GHz on baseline OE–YJ. The left and right plots are given for RR and LL circular polarizations, respectively. No fringes were detected at frequencies from 10.2 to 10.6 GHz. The RFI seen in this frequency band originates at the RAEGYEB antenna.

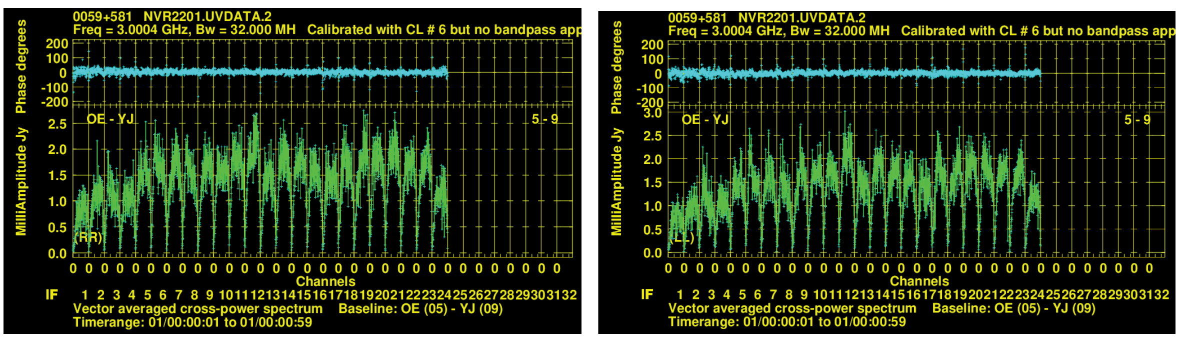

(a) (b)

Fig. 3 Results of global fringe fitting of source '0059+581' for a one-minute scan (same scan as Figure 2) from 3 to 10.6 GHz for baseline OE–YJ. The results are given for RR (left plot) and LL (right plot) polarization. The failure of solutions at frequencies 10.2 to 10.6 GHz is attributed to the low SNR that originated at RAEGYEB.

6.39 GHz, 6.55 GHz, 6.71 GHz, 10.23 GHz, and 10.39 GHz. We also removed spectral windows 43-44, 63-64, 83-84, 103-104, and 123-124 at 3.06 GHz, 5.30 GHz, 6.42 GHz, and 10.26 GHz. Furthermore, we excluded spectral windows 27-28, 47-48, 67-68, 87-88, and 107-108 at 3.29 GHz, 3.45 GHz, 5.53 GHz, 5.69 GHz, 6.65 GHz, 6.80 GHz, 10.49 GHz, and 10.65 GHz. Finally, spectral windows 15-16, 35-36, 55-56, 75-76, 95-96, and 115-116 were removed at 3.42 GHz, 5.27 GHz, 5.65 GHz, 6.77 GHz, and 10.62 GHz. The second stage of flagging involved removing phase cal tones adjacent to the values flagged in the first stage. Additionally, spectral windows 126 to 127 were removed at the following frequencies: 3.03 GHz, 3.19 GHz, 3.35 GHz, 3.45 GHz, 5.27 GHz, 5.30 GHz, 5.43 GHz, 6.39 GHz, 6.65 GHz, 6.71 GHz, 6.77 GHz, and 6.80 GHz.

After the extensive and careful flagging of the phase cal tones in antenna OE, we ran VLBATECR to correct the dispersive delay using JPL maps of total electron content. Next, we applied instrumental phase corrections by executing the VLBAMPCL task. We used the latest flagging table and selected the VGOS source '0059+581' as the calibrator because it exhibited good fringes (see Figure 2) and was observed by all participating antennas except antenna HB. Following this, we applied parallactic angle corrections by running the VLBAPANG task.

Global fringe fitting was performed on all 176 sources to determine the group delays and phase rates. At this stage, the sources were assumed to be point-like. We used the latest calibration table generated, the last flagging table, a signal-to-noise (SNR) threshold of 3, and GS as the reference antenna, and

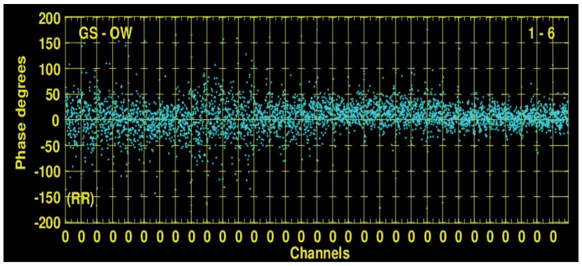

(a)

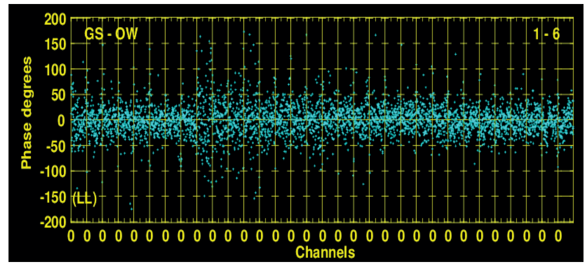

(b)

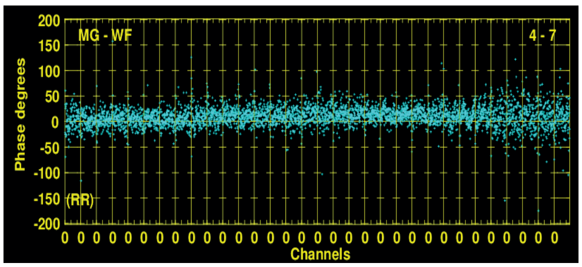

(c)

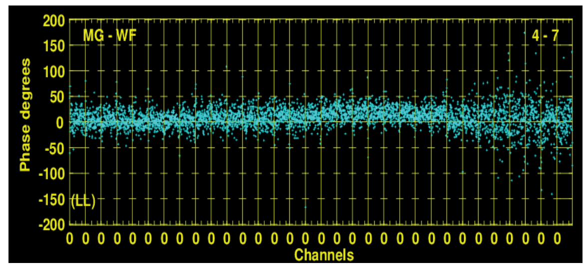

(d)

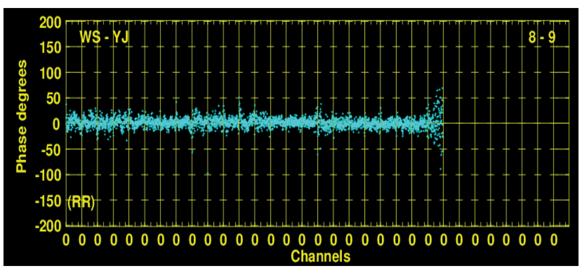

(e)

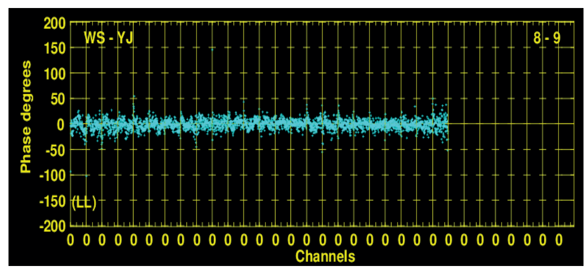

(f)

Fig. 4 Results of global fringe fitting of source '0059+581' for a one-minute scan (same scan as Figure 3) from 3 to 10.6 GHz for both RR (left plot) and LL (right plot) polarization. The failure of solutions at frequencies 10.2 to 10.6 GHz is attributed to the low signal-to-noise ratio (SNR) that originated at RAEGYEB.

we also included a list of multiple reference antennas. The 32 channels were grouped into four bands to fit multi-band group delay (at each band). FRING solutions were then applied to the same sources using task CLCAL. Examples of fringe fitting solutions are shown in Figure 3 for baseline OE-YJ and in Figure 4 for other baselines. No fringe solutions were found in band D for antenna YJ. Finally, bandpass calibration was conducted by running task BPASS, using ten selected sources as calibrators and applying Gaussian spectral smoothing after the calibration. An example of bandpass calibration for antenna WF is displayed in Figure 5.

3 Discussion

We have shown that the global fringe fitting works well for VGOS observations, although it does not necessarily work for all baselines and scans, despite the flagging of bad visibilities. In radio astronomy, a conservative value of a small percentage ($< 10\%$) of fringe-fitting failed solutions is often acceptable. We are investigating the causes of producing failed fringe solutions, which were 13% of the total. The slightly higher percentage of failed solutions we report here might be related to the choice of the reference antenna and to the low SNR between 10.2 GHz and 10.6 GHz at antenna YJ. Additionally, we note that a good bandpass calibration is not obtained without flagging phase cal tones on one of the Onsala antennas.

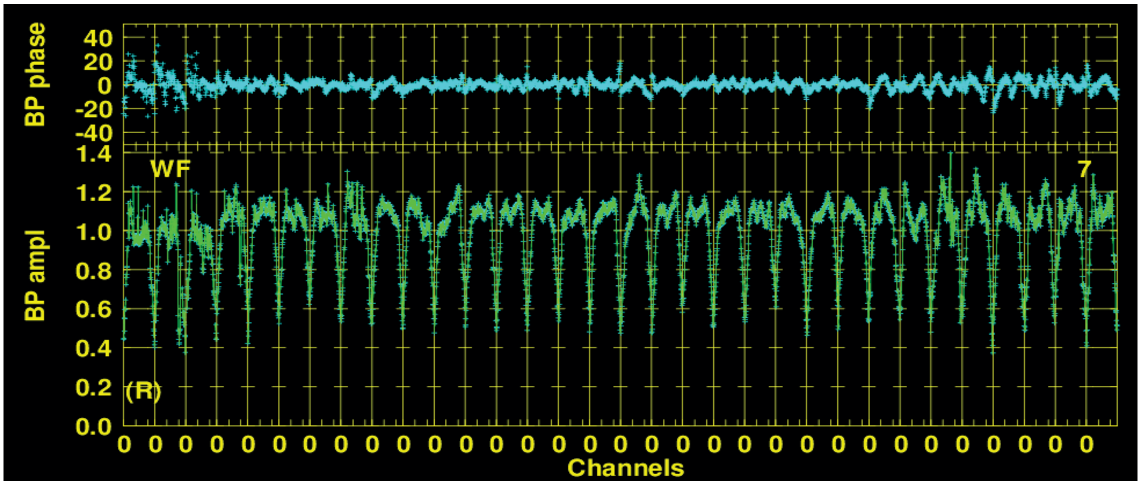

Fig. 5 Bandpass shape from 3 to 10.6 GHz for antenna WF with the R polarization. Top: phase (in units of degrees). Bottom: amplitude.

Because Astrogeodesy aims at modelling the source structure in VGOS observations routinely, it is important that similarly to astronomical VLBI observations, VGOS observes several sources with long scan lengths (of a few minutes) as calibrators needed for instrumental phases (aligning the phases across various channels) and bandpass calibrations. Additionally, if future VGOS observations provide TSYS information, this will enable a standard calibration of VGOS datasets. The value of this is that both phase and amplitude calibrations are fundamental for obtaining a good image dynamic range to resolve the source structure and source flux density estimations, which are also useful for AGN jet research. Furthermore, core-shift measurements in VGOS sources will also be necessary for the future, given that the core-shift time variability can affect the high-accuracy astrometric VLBI measurements of radio sources as discussed by, e.g., [2].

Acknowledgements

This research is supported by the ERC project 101076060.

References

1. Anderson, J. M. and Xu, M. H. (2018) Source Structure and Measurement Noise Are as Important as All Other Residual Sources in Geodetic VLBI Combined. *Journal of Geophysical Research (Solid Earth)* 123(11):10,162-10,190.
2. Chamani, W., Savolainen, T., Ros, E., Kovalev, Y. Y., Wilk, K., Lähteenmäki, A., Tornikoski, M., and Tammi, J. (2023) Time variability of the core-shift effect in the blazar 3C 454.3. A&A, 672:A130.
3. Greisen, E. W. (2003) AIPS, the VLA, and the VLBA. In Heck, A., editor, *Information Handling in Astronomy – Historical Vistas* volume 285 of *Astrophysics and Space Science Library*, page 109.
4. Martí-Vidal, I., Roy, A., Conway, J., and Zensus, A. J. (2016) Calibration of mixed-polarization inferometric observations. Tools for the reduction of inferometric data from elements with linear and circular polarization receivers. A&A, 587:A143.
5. Schartner, M., Collioud, A., Charlot, P., Xu, M. H., and Soja, B. (2023) Bridging astronomical, astrometric and geodetic scheduling for VGOS. *Journal of Geodesy*, 97(2):17.
6. Xu, M., Anderson, J. M., Heinkelmann, R., Lunz, S., Schuh, H., and Wang, G. L. (2019) Structure Effects for 3417 Celestial Reference Frame Radio Sources. ApJS, 242(1):5.
7. Xu, M., Savolainen, T., Zubko, N., Poutanen, M., Lunz, S., Schuh, H., and Wang, G. L. (2021) Imaging vgos observations and investigating source structure effects. *Journal of Geophysical Research: Solid Earth*, 126(4).